Supporting Information

White-Light Defect Emission and Enhanced Photoluminescence Efficiency in 0D Indium-Based Metal Halide

Qidi Ran, Yan Zhang, Jun Yang, Rongxing He,* Lei Zhou,* and Shanshan Hu*

Key Laboratory of Luminescence Analysis and Molecular Sensing (Southwest University), Ministry of Education, School of Chemistry and Chemical Engineering, Southwest University, Chongqing 400715, PR China

Corresponding Authors

*herx@swu.edu.cn

*zhoulei25@swu.edu.cn

*hushan3@swu.edu.cn

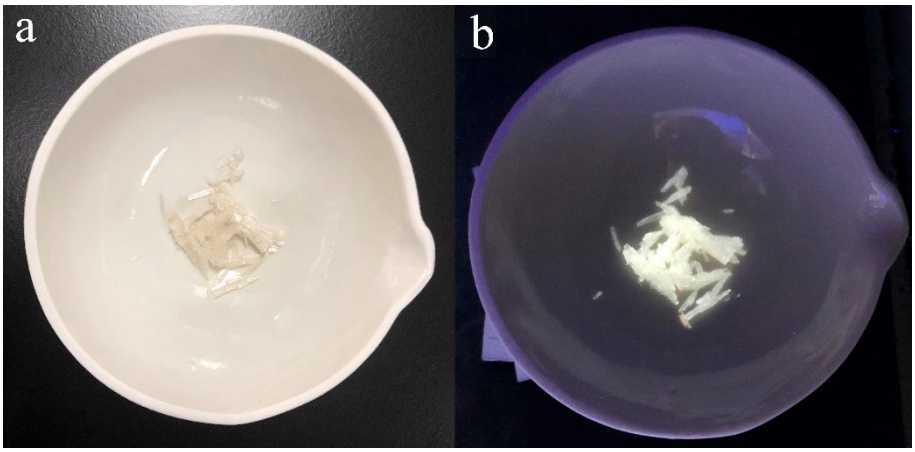

Figure S1. Photographs of $(C_6H_8N)_6InBr_9$ crystals under nature light (a) and 365 nm UV light (b).

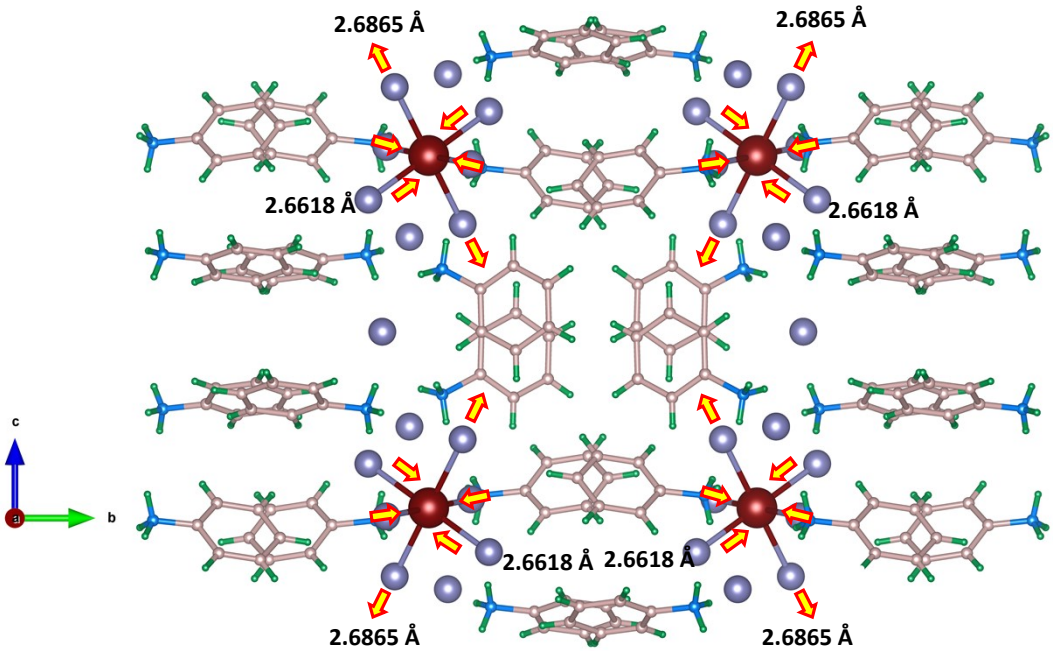

Figure S2. Detailed view of the structure of $(InBr_6)^{3-}$ octahedron that exhibits a Jahn-Teller-like distortion.

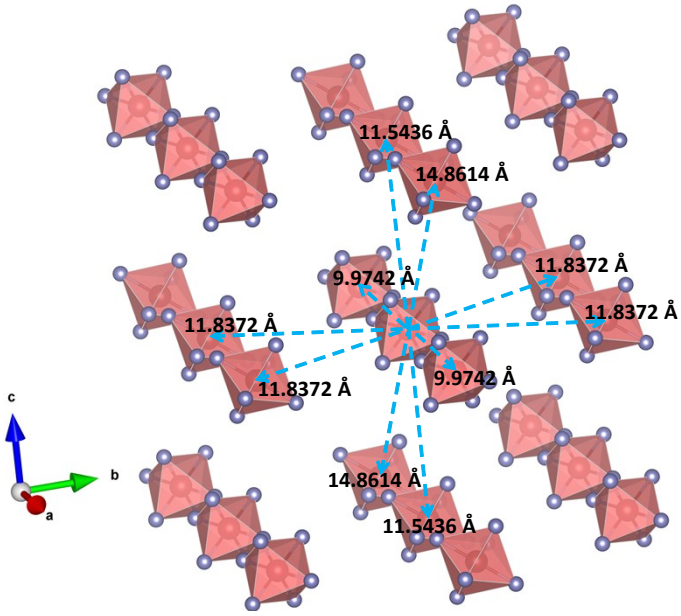

Figure S3. Distance between the adjacent In atom.

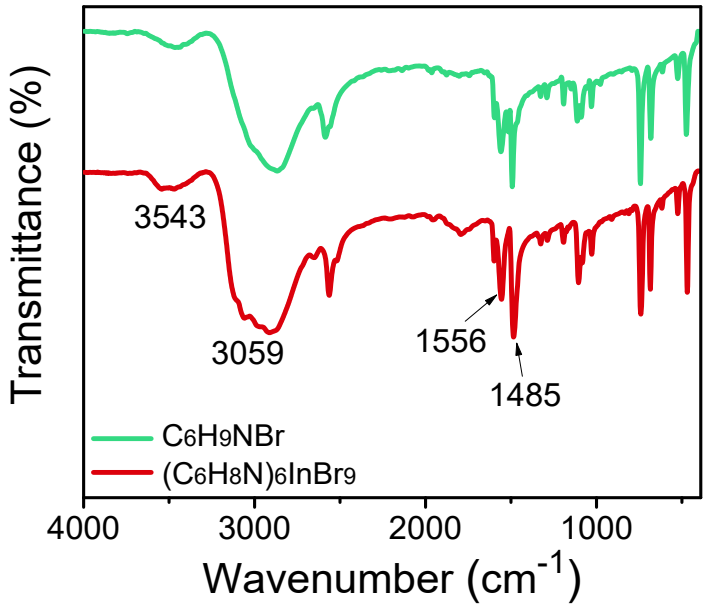

Figure S4. FTIR spectra of C_6H_9NBr and $(C_6H_8N)_6InBr_9$.

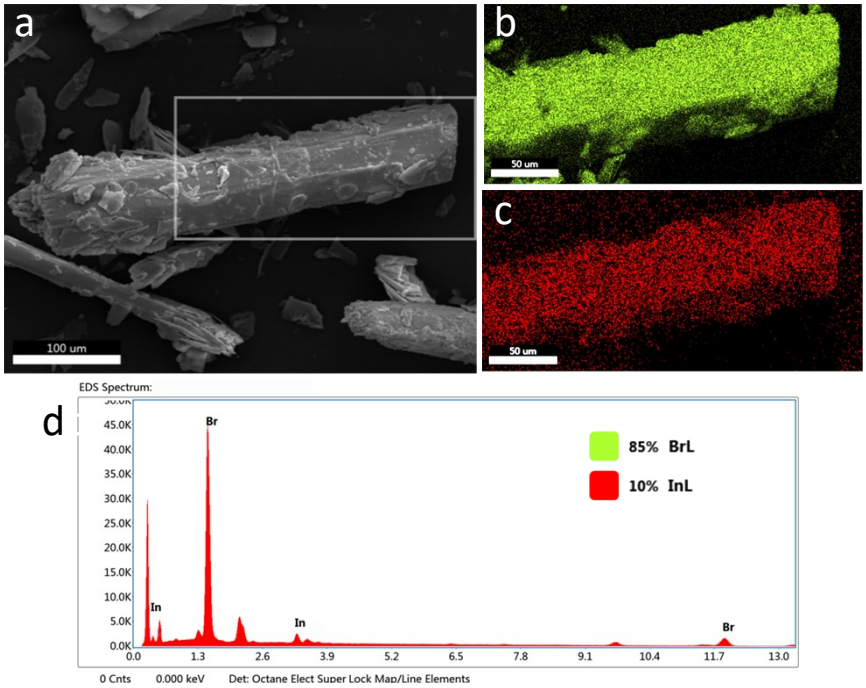

Figure S5. (a) Scanning electron microscope (SEM) image of $(C_6H_8N)_6InBr_9$ single crystals. (b) and (c) is the corresponding EDX mapping of In and Br element, respectively. (d) Representative EDX spectrum of $(C_6H_8N)_6InBr_9$ crystal. The Br:In ratio is 8.5:1, slightly lower than 9:1 which is the theoretical ratio for $(C_6H_8N)_6InBr_9$.

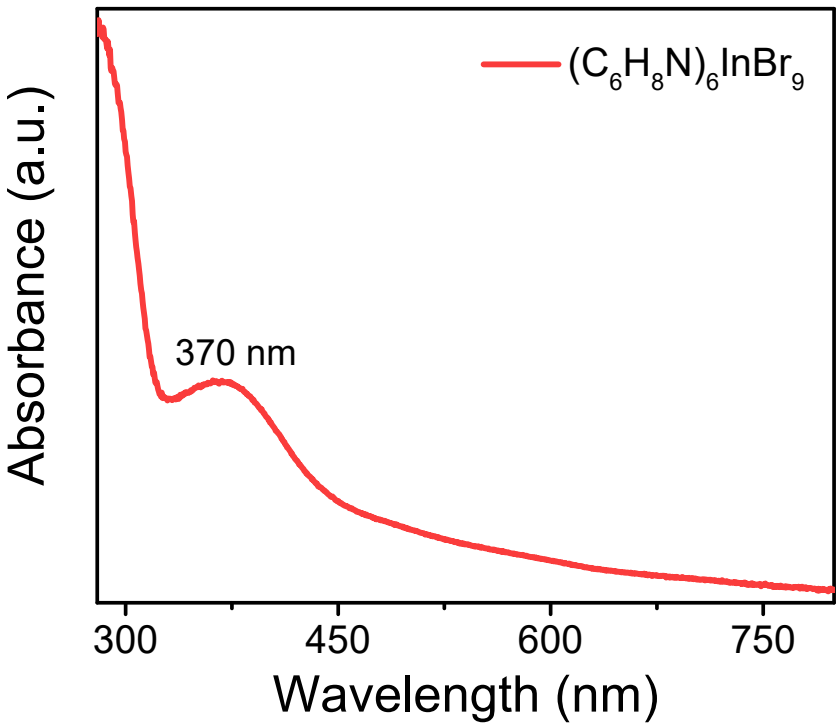

Figure S6. UV-vis absorption spectrum of $(C_6H_8N)_6InBr_9$.

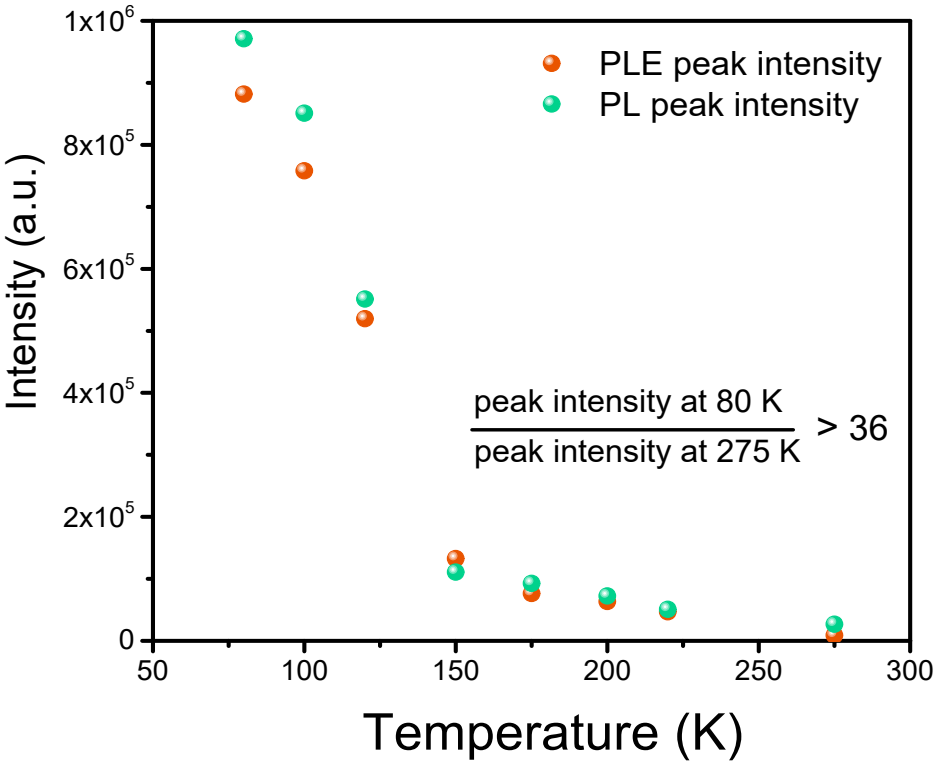

Figure S7. PLE/PL peak intensities of $(C_6H_8N)_6InBr_9$ at different temperature.

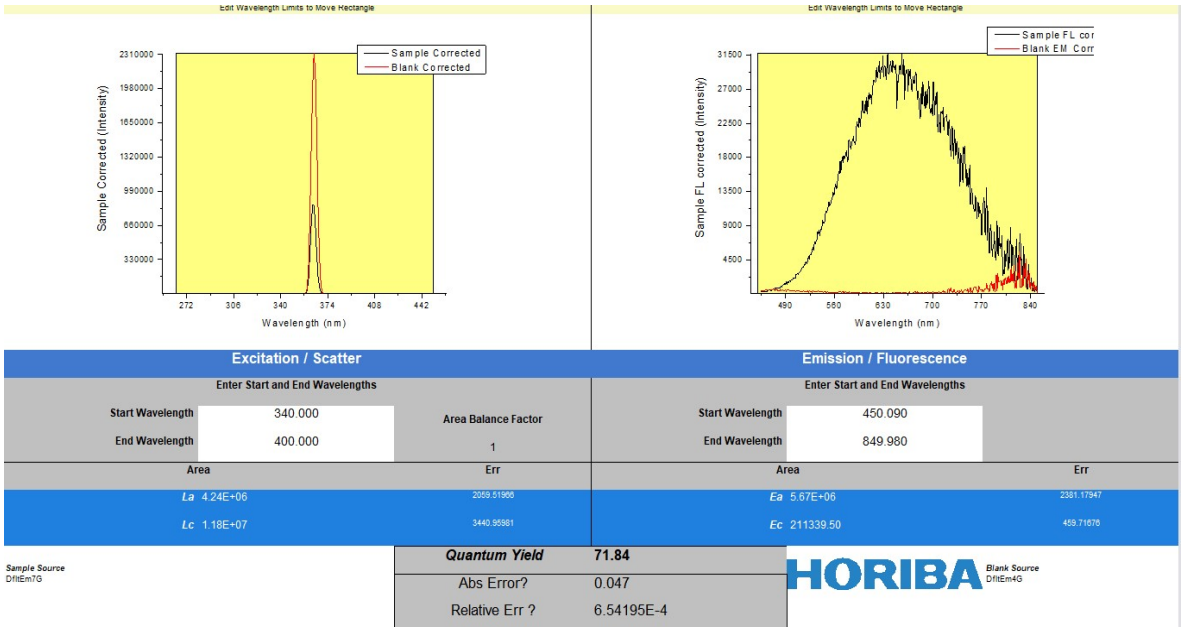

Figure S8. The measured PLQY value of $(C_6H_8N)_6InBr_9$:0.58%Sb.

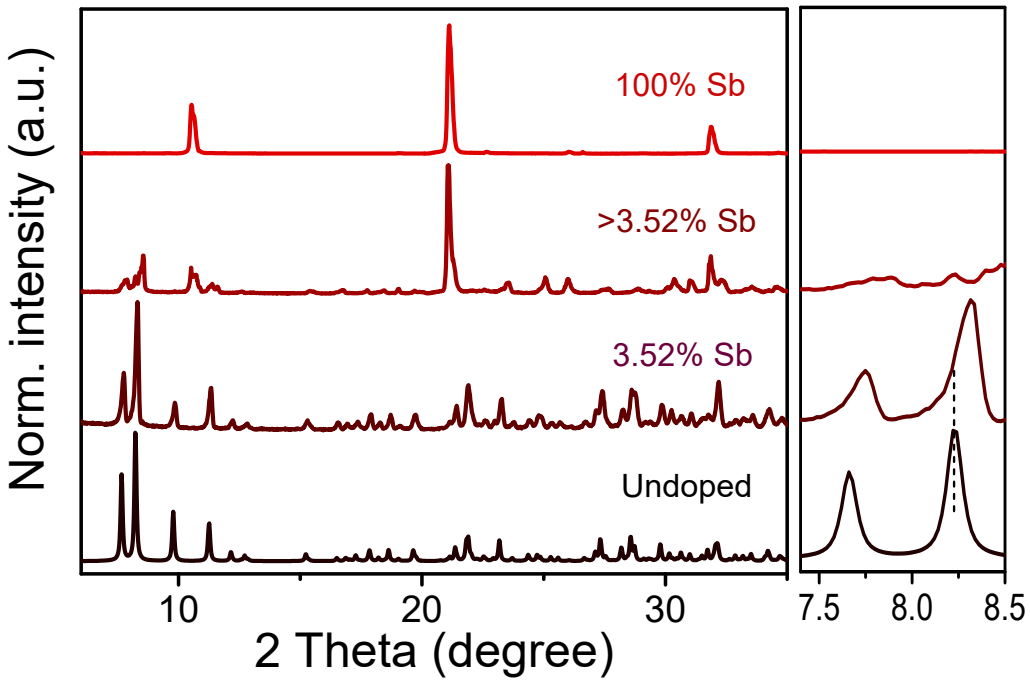

Figure S9. PXRD patterns of Sb^{3+}-doped $(C_6H_8N)_6InBr_9$ with Sb^{3+} amount from 3.52% to 100%. The right part displays the selected range, where the PXRD peaks have moved toward higher diffraction degrees.

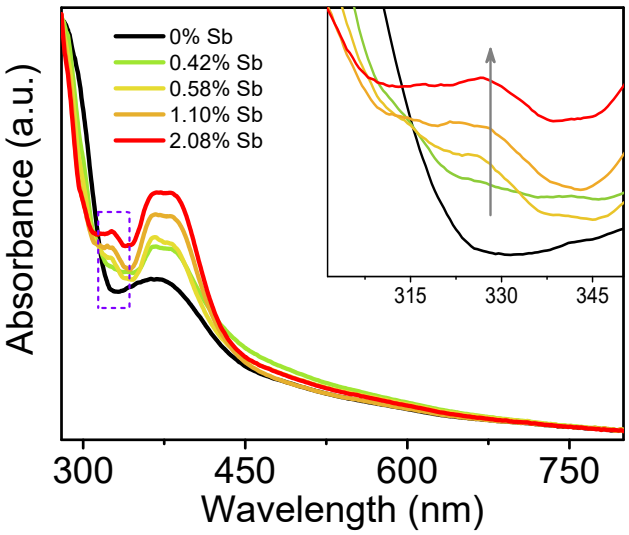

Figure S10. UV-vis absorption spectra of $(C_6H_8N)_6InBr_9$:x%Sb (x = 0 ~ 2.08). The inset shows the selected range, where an additional absorption peak between 315 and 340 nm emerges and enhances with increasing Sb^{3+} amount, which can be attributed to the $^1S_0 \rightarrow {}^3P_1$ transition of Sb^{3+}.

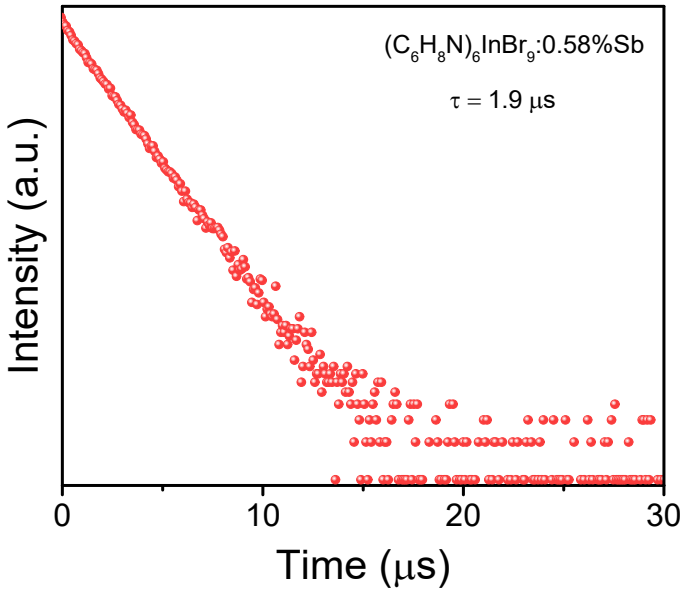

Figure S11. PL decay curve of $(C_6H_8N)_6InBr_9$:0.58%Sb measured at 645 nm.

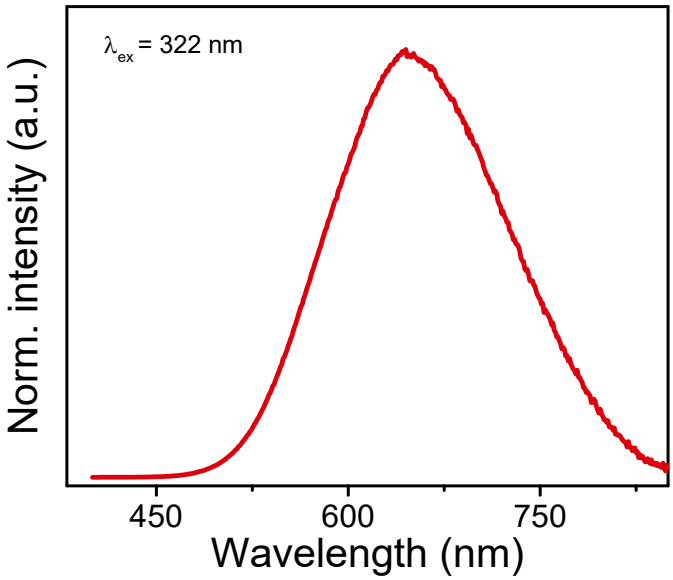

Figure S12. PL spectrum of $(C_6H_8N)_6InBr_9$:0.58%Sb by exciting at 322 nm.

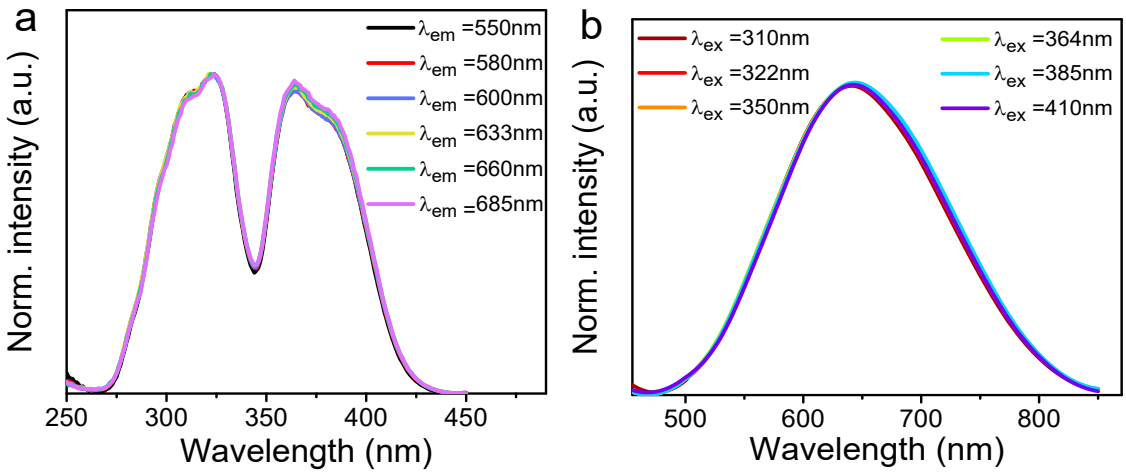

Figure S13. Emission-wavelength-dependent photoluminescence excitation (PLE) spectra (a) and Excitation-wavelength dependent PL spectra (b) of $(C_6H_8N)_6InBr_9$:0.58%Sb.

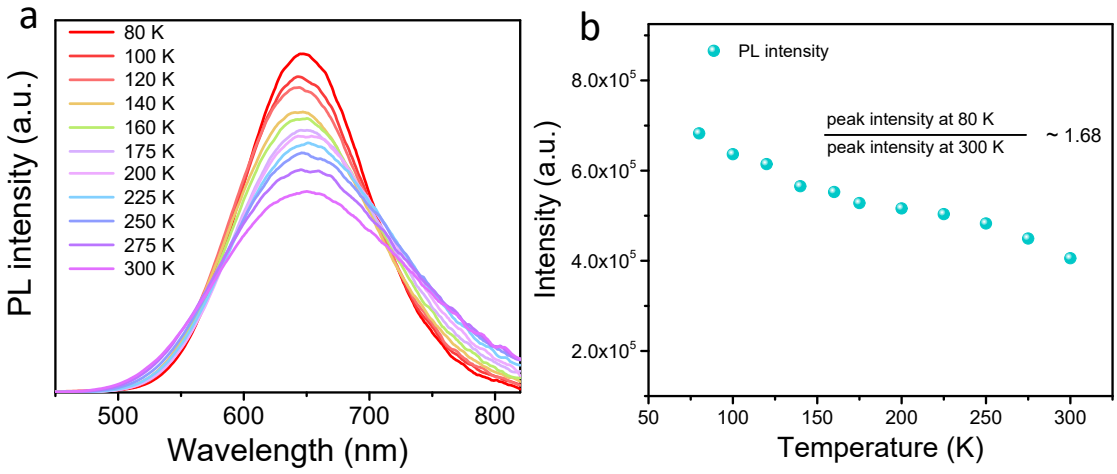

Figure S14. (a) Temperature-dependent PL spectra of $(C_6H_8N)_6InBr_9$:0.58%Sb. (b) PL peak intensities at different temperature.

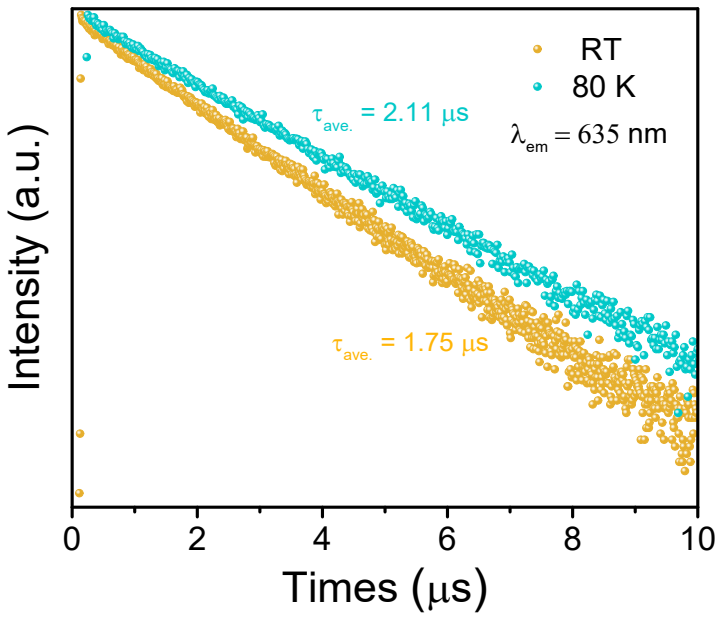

Figure S15. PL decay curves of $(C_6H_8N)_6InBr_9$:0.58%Sb measured at RT (blue dots) and 80 K (yellow dots).

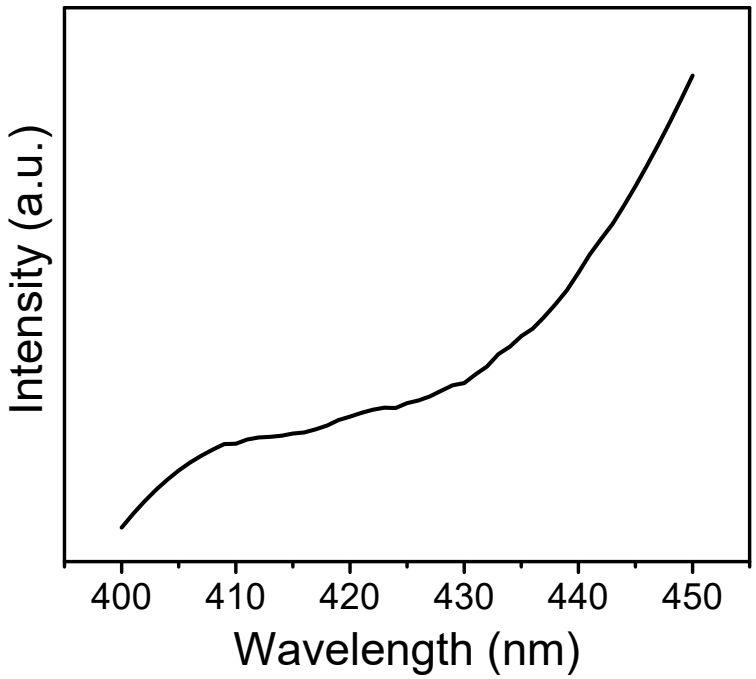

Figure S16. PL spectrum of $(C_6H_8N)_6InBr_9$:0.58%Sb in the range from 400 to 450 nm, in which almost no defect-related emission can be detected.

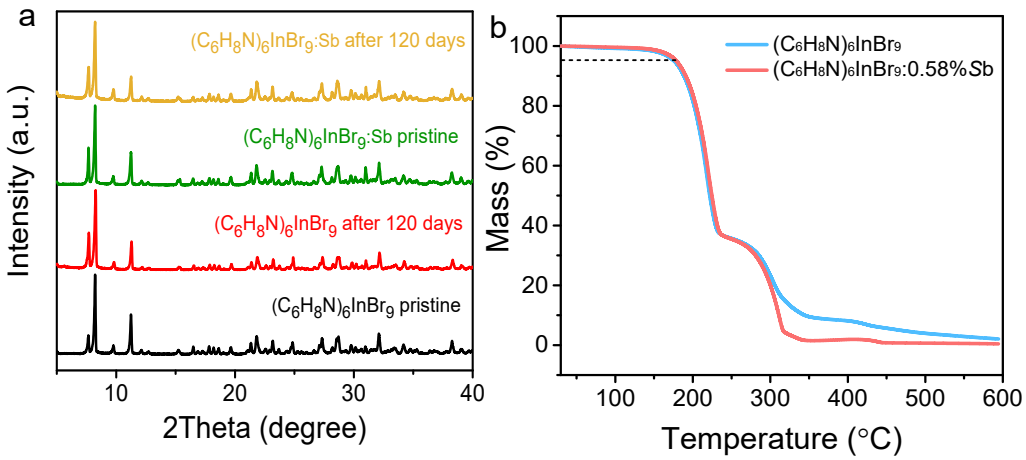

Figure S17. (a) PXRD patterns of $(C_6H_8N)_6InBr_9$ and $(C_6H_8N)_6InBr_9$:0.58%Sb stored in different periods. (b) Thermogravimetric analysis (TGA) thermogram of $(C_6H_8N)_6InBr_9$ and $(C_6H_8N)_6InBr_9$:0.58%Sb.

Table S1. Single crystal X-ray diffraction data of $(C_6H_8N)_6InBr_9$ single crystal.

Compound	$(C_6H_8N)_6InBr_9$
Formula weight (g/mol)	1397.82
Temperature (K)	296
Crystal system	monoclinic
Space group	I2/a
a (Å)	9.9742(2)
b (Å)	21.4709(4)
c (Å)	23.0872(4)
α (°)	90
β (°)	92.957(2)
γ (°)	90
Volume(Å^3)	4937.66(16)
Z	4
Radiation	Cu Kα (λ = 1.54184)
ρcalc. (g/cm^3)	1.880
μ (mm^{-1})	12.597
F(000)	2676.0
Crystal size/mm3	0.2 × 0.02 × 0.02
Index ranges	-6 ≤ h ≤ 12, -25 ≤ k ≤ 24, -28 ≤ l ≤ 28
Data collection range	5.627° < θ < 71.544°
Data completeness	0.9962
R indexes [I>=2σ (I)]	R_1 = 0.0415, wR_2 = 0.1119
Independent reflections	4715[R_{int} = 0.0178, R_{sigma} = 0.0255]
Data/Parameters	4715/390/340
Goodness-of-fit on F^2	1.036
Largest diff. peak and hole (eÅ^3)	1.95 and -0.66

Table S2. Fitting parameters for the PL decay curves of $(C_6H_8N)_6InBr_9$ using a three-exponential decay model.

Emission wavelength (nm)	Lifetime (ns)	τ_1 (ns)	τ_2 (ns)	τ_3 (ns)
423	1.07	1.22(41%)	0.28(47%)	3.72(12%)
450	1.21	1.52(41%)	0.32(49%)	4.41(10%)
500	1.78	2.36(42%)	0.53(52%)	8.92(6%)
545	2.02	2.35(44%)	8.65(9%)	0.53(47%)
575	1.96	2.25(45%)	8.03(9%)	0.48(46%)

Table S3. A comparison of the PL properties between Sb^{3+}-doped $(C_6H_8N)_6InBr_9$ and other lead-containing compounds.

Compound	**PL (nm)**	**fwhm (nm)**	**CIE**	**PLQY (%)**	**Reference**
(EDBE)[$PbBr_4$]	573	215	(0.39, 0.42)	9	J. Am. Chem. Soc. 2014, 136,13154-13157
(N-MEDA)[$PbBr_4$]	558	165	(0.36,0.41)	~0.5	J. Am. Chem. Soc. 2014, 136, 1718-1721
(2meptH_2)$PbBr_4$	417	-	(0.24, 0.23)	3.37	Chem. Commun., 2018, 54, 4053--4056
$(C_{13}H_{19}N_4)_2PbBr_4$	460	66	(0.14, 0.09)	~40	ACS Materials Lett. 2019, 1, 594−598
$(C_5H_{14}N_2)_2Pb_4MnCl_{14}$	678	-	(0.68, 0.31)	32	J. Am. Chem. Soc. 2019, 141, 12197−12201
(benzyl)$_6$[Pb_3Br_{12}]	571	146	(0.43, 0.50)	10	Chem. Mater. 2020, 32, 4431−4441
$(C_9H_{22}N_2)PbBr_4$	620	100	(0.56, 0.37)	4.7	J. Phys. Chem. Lett. 2020, 11, 2934−2940
(TDMP)$PbBr_4$: 0.027%Mn	510/ 640	-	(0.33, 0.37)	60	Angew. Chem. 2020, 132, 2824 – 2829
(N-AEP)$_2Pb_2Cl_{10}\cdot H_2O$	396/ 493	-	(0.31, 0.33)	1	J. Mater. Chem. C, 2020, 8, 6710—6714
[BAPrEDA]$PbCl_6\cdot(H_2O)_2$	392	73	(013, 0.11)	21.3	J. Mater. Chem. C, 2020, 8, 11890--11895
[TMPDA]$_2Pb_3Br_{10}$	526	25	(0.16, 077)	71.95	J. Mater. Chem. C,2021, 9, 15047-15055
[DTHPE]$_2Pb_3Cl_{10}$	445	174	(0.25, 0.29)	19.45	Chem. Commun., 2021, 57, 1218--1221
$(C_6H_8N)_6InBr_9$: 0.58%Sb	645	165	(0.57, 0.42)	71.84	**This work**

Table S4. PLQYs of Sb^{3+}-doped $(C_6H_8N)_6InBr_9$ with different Sb^{3+} amount.

Molar ratio	PLQY (%)
< 0.42	29.84
0.42%	37.60
0.58%	71.84
1.10%	57.73
2.08%	42.38
3.52%	41.31

Table S5. Elemental analysis (by ICP-OES) of Sb^{3+}-doped $(C_6H_8N)_6InBr_9$ with different Sb^{3+} amount.

Molar ratio	Sb (μg/mL)	In (μg/mL)
0.42%	0.046	10.35
0.58%	0.064	10.44
1.10%	0.124	10.58
2.08%	0.226	10.24
3.52%	0.398	10.65

Table S6. Summary of Huang-Rhys factor (S)

Compounds	Huang-Rhys factor (S)	Reference
$Rb_7Sb_3Cl_{16}$	9.6	Sci. Bull. 2019, 64, 904
(MA)4Cu2Br6	10.7	J. Phys. Chem. Lett. 2020, 11, 4703
$(BzTEA)_2TeCl_6$	12.45	J. Mater. Chem. C, 2021, 9, 4351-4358
13%Mn:$CsCdBr_3$	11	J. Phys. Chem. C 2021, 125, 32, 18031
$(TBA)CuCl_2$	8.46	J. Phys. Chem. Lett. 2021, 12, 6919
$(TBA)CuBr_2$	14.38	
$ODASnBr_4$ [16%-DCM]	27.5	Adv. Funct. Mater. 2021, 2102182
$ODASnBr_4$ [70%-CFM]	26.0	
Cs_2ZrCl_6:Te	26.93	J. Energy Chem. 2022, 65, 600

Cs_2NaYCl_6	7.0	Phys. Rev. B 1986, 34, 2735
$Cs_2AgInCl_6$	37	Nature 2018, 563, 541-545
$Cs_2InCl_5 \cdot H2O:Sb^{3+}$	32.28	Chem. Mater. 2020, 32, 12, 5327-5334
$(C_6H_8N)_6InBr_9$:0.58%Sb	31.16	**This work**